J. Fluid Mech. (1995), *vol.* 301, *pp.* 109–132

Analytical description of the breakup of liquid jets

By DEMETRIOS T. PAPAGEORGIOU

Department of Mathematics and Center for Applied Mathematics and Statistics,
New Jersey Institute of Technology, Newark, NJ 07102, USA

(Received 27 October 1994 and in revised form 1 June 1995)

A viscous or inviscid cylindrical jet with surface tension in a surrounding medium of negligible density tends to pinch owing to the mechanism of capillary instability. We construct similarity solutions which describe this phenomenon as a critical time is encountered, for three distinct cases: (i) inviscid jets governed by the Euler equations, (ii) highly viscous jets governed by the Stokes equations, and (iii) viscous jets governed by the Navier–Stokes equations. We look for singular solutions of the governing equations directly rather than by analysis of simplified models arising from slender-jet theories. For Stokes jets implicitly defined closed-form solutions are constructed which allow the scaling exponents to be fixed. Navier–Stokes pinching solutions follow rationally from the Stokes ones by bringing unsteady and nonlinear terms into the momentum equations to leading order. This balance fixes a set of universal scaling functions for the phenomenon. Finally we show how the pinching solutions can be used to provide an analytical description of the dynamics beyond breakup.

1. Introduction

It is well known (Rayleigh 1879), that a circular jet of finite radius with a surface which supports surface tension is linearly unstable to a long-wave capillary instability. Any small perturbations with wavelengths larger than the jet radius grow exponentially. Furthermore, linear theory predicts a maximally growing wave and hence a dominant length scale for the instability. According to linear theory, then, the dominant wavelength is approximately $9a$ where a is the unperturbed jet radius. (This result is independent of the surface tension coefficient.) Experiments indicate that the instability can lead to breakup, or pinching, of the jet into drops. Clearly the pinching phenomenon is nonlinear since the initial disturbance has to grow to amplitudes of the order of the unperturbed jet radius. Linear theory, however, does well in the qualitative prediction of breakup times, for instance, by employment of empirical arguments such as e-fold amplification of perturbations. In many applications the shape and jet velocities at breakup are useful but cannot be obtained from linear theory. This classical problem has been studied extensively; experiments have been carried out by Donnelly & Glaberson (1966), Goedde & Yuen (1970) and more recently Chaudhary & Maxworthy (1980*a*, *b*). An experimental investigation of capillary instability of a dripping jet has been carried out by Peregrine, Shoker & Symon (1990) where many photographs of the breaking phenomenon are found. Of particular interest are the fine details captured beyond pinching which include ripples on the surface of the jet away from the pinch region. Weakly nonlinear theories (see below) have been carried out by Yuen (1968) and later by Chaudhary & Redekopp (1980). A review of the subject can be found in Bogy (1979) while recent simulations using boundary integral techniques are described in Mansour & Lundgren (1990).

Viscous-dominated flows form a separate but parallel field. Tomotika (1936) considered the linear stability of a stationary cylindrical thread of viscous fluid surrounded by a second viscous fluid with surface tension acting at the interface. Qualitatively, the stability results are similar to inviscid studies with a maximally growing wave with wavelength of the order of the unperturbed thread radius. A more complete theory, including the effects of non-uniform jet velocities, can be found in Chandrasekhar (1961), where it is shown that capillary instability provides linearly growing waves that scale on the jet radius. Recently, Tjahjadi, Stone & Ottino (1992), have undertaken an experimental and numerical study of the breakup of viscous cylindrical threads of one fluid in another. The experiments and the computations show that at the time of breakup the jet tends to form larger mother drops joined to smaller satellite drops by thin slender tubes.

The present approach is a fully nonlinear one with interfacial deflections as large as the undisturbed jet radius, as opposed to most previously weakly nonlinear studies. Chaudhary & Redekopp (1980) (see also Yuen 1968) consider two low-amplitude (asymptotically small but not infinitesimally so) initial perturbations, a fundamental and a harmonic. These are followed up to cubic order in the initial small amplitude, which is the first stage when the modes interact nonlinearly to produce an amplitude equation. The methodology is that of the Stuart (1960) and Watson (1960) classical weakly nonlinear theory, even though the jet problem always has a band of unstable waves which does not become monochromatic as a flow parameter (e.g. capillary number here) is varied. The results are therefore valid for sufficiently small times, but as Chaudhary & Redekopp indicate, qualitative features of the experiments are reproduced at times which seem to be beyond the validity of the theory. Fully nonlinear theories allow the interfacial amplitude to be as large as the unperturbed jet radius, a situation which is essential in the description of breakup. This usually means that the problem should be addressed numerically, and it is the objective of this work to present an analysis of breakup.

A fully nonlinear theory of inviscid jet breakup in a vacuum was developed by Ting & Keller (1991, referred to herein as TK). A set of one-dimensional evolution equations was derived by an asymptotic expansion procedure which used the ratio between undisturbed jet radius and characteristic axial length scale as a small parameter. The equations were used to find similarity solutions at times just after (or just before) pinching and to use them along with a mass and momentum balance (see also Keller 1983) to form a description of the dynamics beyond pinching. An essential element in this construction is the choice of the scaling exponent in the similarity solution. Since the slender-jet theory does not fix this scaling exponent, a family of solutions depending on the scaling parameter is given. The breakup of a fluid sheet (two-dimensional) is also considered in TK and earlier by Keller & Miksis (1983). The latter study does not assume slenderness and follows the dynamics just beyond breakup by constructing numerical solutions of a self-similar system of equations arising from the Euler equations. The analogous system in cylindrical geometries is given by us in §2.2.

The construction of similarity solutions in TK proceeds in two steps: first a reduced set of one-dimensional equations is developed using a slender-jet approximation, and second, pinching solutions of these equations are found. Our approach differs in that the two steps are combined into one with the slenderness ratio being time-dependent and becoming asymptotically zero as the postulated singular time is approached. It is not surprising, then, that the results for inviscid jets are identical to those in TK. Our main interest is in viscous jets but the method is briefly described for inviscid jets also to show consistency with the work of TK. A qualification needs to be made, however.

The two-step approach provides a simplified evolution system that may not capture correctly the transient flow which precedes pinching. In fact, as is briefly discussed in §2, for inviscid jets numerical solutions of the initial value problem on periodic domains suggest that an infinite slope singularity is encountered before the minimum jet radius vanishes; this in turn implies that the long-wave assumption is violated and for the periodic boundary conditions utilized in the numerical experiments, the pinching self-similar structure supported by the one-dimensional equations does not appear as a terminal state. It is worth noting that one-dimensional models of viscous jets do not encounter infinite slope singularities (for periodic boundary conditions also) as is evidenced by the work of Eggers & Dupont (1994) and Eggers (1993, 1995) for viscous jets with inertia and by Papageorgiou (1995) for Stokes jets.

The dynamics of slender viscous jets have been studied recently by reduction of the equations of motion to one-dimensional models. Renardy (1994) considered viscoelastic and Newtonian jets governed by Stokes equations; he shows analytically that viscoelastic jets under several constitutive laws remain free of finite-time singularities while Newtonian jets break after a finite time under certain assumptions. Analogous models of jets governed by the Navier–Stokes equations have been derived by Eggers (1993) (see also Eggers & Dupont 1994; Eggers 1995 and Papageorgiou 1994). These one-dimensional models allow universal similarity solutions at pinching.

The objective of this work is to look for singular solutions directly from the equations, as in the work of TK, but without first deriving one-dimensional equations. If the slenderness assumption is valid at the time of pinching, it is shown that self-similar pinching solutions of the two approaches are equivalent. Navier–Stokes solutions follow by a rational extension of the results for Stokes jets and both are analysed before and after pinching. The dynamics after pinching involve mass and momentum balances of the motion of a blob of fluid attached to the end of the slender jet; such analysis was first performed by Keller (1983) and extended by TK to include the effect of the flow in the adjoining thread of fluid; more recently Keller, King & Ting (1995) have analysed blob formation by incorporating into the previous models the flow inside the blob – this involves solving the Euler equations in a non-slender but spherical geometry with matching effected with the adjoining thread of fluid. Scaling exponents can be fixed for viscous slender jets while for inviscid jets the theory is generalized to non-slender pinching configurations in order to achieve this. The axisymmetric analogue of the problem solved by Keller & Miksis (1983) needs to be addressed for inviscid flows, then.

The article is organized as follows. Section 2 deals with the breakup of inviscid jets governed by the axially symmetric Euler equations. The theory is generalized to non-slender configurations in order to fix the scaling exponents, and the governing system in such instances is derived. Section 3 considers jets described by the Stokes equations. Self-similar equations are derived near the pinching time and solved and the scaling functions are determined. The exponents are universal but the scaling functions contain an arbitrary multiplicative constant. In §4 the inertial and unsteady terms dropped in the derivation of the Stokes flow are retained and a system governing the local flow in this case is derived and analysed. In §5 we use the solutions at pinching for both Stokes and Navier–Stokes jets to construct the dynamics beyond the pinch point. In the latter case the local description is free of arbitrary constants.

2. The theory for inviscid jets

The equations governing the fluid motion can be written in terms of a velocity potential $\phi(t, r, z)$ which is independent of the azimuthal angle θ for axisymmetric flows. A system of cylindrical polar coordinates (r, θ, z) is used with corresponding velocity vector $\boldsymbol{u} = (u, v, w) = \nabla\phi$. Using this notation, ϕ satisfies Laplace's equation while at the free surface two conditions are specified: a kinematic condition and a normal stresses balance which gives the pressure jump across the interface. When the latter condition is used in the z-momentum equation the usual Bernoulli equation arises. Without loss of generality we give the system for a static undisturbed jet, noting that any background axial velocity can be removed by a Galilean transformation. The equations with boundary conditions are

$$\phi_{rr} + \frac{1}{r}\phi_r + \phi_{zz} = 0; \tag{2.1a}$$

on $r = S(t, z)$

$$\phi_r = S_t + \phi_z S_z, \tag{2.1b}$$

$$\phi_t + \tfrac{1}{2}(\phi_r^2 + \phi_z^2) = -\left(\frac{1}{S} - S_{zz} + \frac{S_z^2 S_{zz}}{1 + S_z^2}\right)(1 + S_z^2)^{-1/2}. \tag{2.1c}$$

A final boundary condition is regularity of ϕ at $r = 0$. Equations (2.1 *a–c*) are in non-dimensional form where the following scalings are used: spatial variables are scaled with R the undisturbed jet radius; the time scale is that of capillary instability and is given by $(\rho R^3/\sigma)^{1/2}$ where ρ is the fluid density and σ the surface tension coefficient (both assumed to be constant); the potential ϕ is scaled by $(R\sigma/\rho)^{1/2}$. These are the classical scalings that lead to Rayleigh's linear stability results.

In general (2.1 *a–c*) must be addressed numerically subject to suitable initial conditions, for instance,

$$\phi(r, z, 0) = \phi_i(r, z), \quad S(z, 0) = S_i(z). \tag{2.2a, b}$$

In what follows we consider the possibility of the jet pinching after a finite time with the radius tending to zero at some point or points. The analysis presented is a local one and does not lead to a prediction of the singular time but provides possible terminal self-similar structures. Two distinct but related cases are analysed. First a slender-jet approach is taken whereby the jet shape near the pinching timer is characterized by a long axial length scale compared to its amplitude, resulting in similarity equations equivalent to those found by analysis of long-wave partial differential equations (as in TK for instance). In the second case the slender-jet scalings are dropped and a theory with solutions with comparable axial and radial length scales is presented (an axisymmetric extension of the problem studied by Keller & Miksis 1983).

2.1. *Slender-jet theory*

We construct pinching solutions of (2.1 *a–c*) by assuming the following ansatz as a singular time t_s is approached from below (in what follows $\tau = (t_s - t)$ unless otherwise stated):

$$r = \tau^\alpha y, \quad z = \tau^\beta \xi, \quad S(t, z) = \tau^\alpha f(\tau, \xi), \tag{2.3a–c}$$

$$\phi(\tau, r, z) = \tau^\gamma \chi(\tau, y, \xi). \tag{2.3d}$$

According to these transformations time and space derivatives become

$$\frac{\partial}{\partial t} \to -\frac{\partial}{\partial \tau} + \frac{\beta\xi}{\tau}\frac{\partial}{\partial \xi} + \frac{\alpha y}{\tau}\frac{\partial}{\partial y}, \quad \frac{\partial}{\partial r} \to \tau^{-\alpha}\frac{\partial}{\partial y}, \quad \frac{\partial}{\partial z} \to \tau^{-\beta}\frac{\partial}{\partial \xi}. \tag{2.3e–g}$$

For slender-jet shapes at breakup, then, we have $r \ll z$ which in turn suggests the condition

$$\alpha > \beta. \tag{2.4}$$

Substitution of the ansatz (2.3*a–g*) into (2.1*a*) converts the Laplace equation into

$$\chi_{yy} + \frac{1}{y}\chi_y + \tau^{2\alpha-2\beta}\chi_{\xi\xi} = 0. \tag{2.5}$$

According to (2.4), $\tau^{2\alpha-2\beta}$ is a small parameter and an expansion for χ can be sought as follows:

$$\chi = \chi_0(y,\xi) + \tau^{2\alpha-2\beta}\chi_1(y,\xi) + \tau^{4\alpha-4\beta}\chi_2(y,x) + \ldots, \tag{2.6}$$

$$f(\tau,\xi) = f_0(\xi) + \tau^{2\alpha-2\beta}f_1(\xi) + \ldots. \tag{2.7}$$

Substitution of (2.6) into (2.5) gives the following solutions to leading order which are regular on the jet axis $y = 0$:

$$\chi_0 = A(\xi), \quad \chi_1 = -\tfrac{1}{4}y^2A_{\xi\xi} + B(\xi), \quad \chi_2 = \tfrac{1}{64}y^4A_{\xi\xi\xi\xi} - \tfrac{1}{4}y^2B_{\xi\xi} + C(\xi), \tag{2.8a–c}$$

where the functions $A(\xi)$, $B(\xi)$, etc. are to be found.

Next we consider the kinematic condition (2.1*b*). Substitution of the ansatz (2.3) into (2.1*b*) along with the expansions (2.6), (2.7) and the solutions (2.8*a*, *b*) yields, to leading
order, the equation (primes denote ξ-derivatives)

$$-\tfrac{1}{2}\tau^{\gamma+\alpha-2\beta}f_0A'' = \tau^{\alpha-1}(-\alpha f_0 + \beta\xi f_0') + \tau^{\gamma+\alpha-2\beta}A'f_0' + O(\tau^{\gamma+3\alpha-4\beta}). \tag{2.9}$$

It can be seen from (2.9) that a leading-order balance arises by

$$\gamma + \alpha - 2\beta = \alpha - 1 \Rightarrow \gamma = 2\beta - 1, \tag{2.10}$$

with (2.9) becoming

$$\tfrac{1}{2}f_0A'' + A'f_0' - \alpha f_0 + \beta\xi f_0' = 0. \tag{2.11}$$

A second equation connecting $A(\xi)$ and $f_0(\xi)$ is found by a leading-order balance in the Bernoulli equation (2.1*c*). Proceeding as above and substituting the value for γ found above, we find to leading order,

$$\tau^{2\beta-2}[(1-2\beta)A + \beta\xi A' + \tfrac{1}{2}(A')^2] = -\tau^{2\beta-2}\frac{1}{f_0} + O(\tau^{2-4\beta}). \tag{2.12}$$

In obtaining (2.12) a leading-order balance has been made which determines α in terms of β:

$$\alpha = 2 - 2\beta. \tag{2.13}$$

Clearly the expansions in the kinematic condition and the Bernoulli equation are consistent if

$$\beta < \tfrac{2}{3}.$$

This is easily found, for example, by comparing the first two terms in (2.12) and using the fact that $\tau \to 0+$. The case $\beta = \frac{2}{3}$ is a critical one and implies that $\alpha = \frac{2}{3}$ also; the slender-jet assumption is no longer valid then, and a different analysis is required (see §2.2 below).

The system to be solved, therefore, is (2.11) along with the leading term of (2.12) which is

$$(1-2\beta)A + \beta\xi A' + \tfrac{1}{2}(A')^2 + \frac{1}{f_0} = 0. \tag{2.14}$$

The coupled system (2.11) and (2.14) determine acceptable scaling functions as a pinch forms in the jet. The value of β is left undetermined by the analysis; a higher-order analysis which includes the effect of higher-order terms in the expansions (2.6) and (2.7) has been carried out in an attempt to obtain further information on β. It has been found (for brevity this is not included here) that higher-order corrections are governed by linear equations with forcings which depend on A and f_0. In particular, second-order corrections are governed by equations which are regular for all values of β of interest and so no additional information is obtained. A slender-jet theory which includes higher-order terms and in particular the axial effect of surface tension is able to fix the value of β but the equations are different, as expected. These results are reported elsewhere.

It is useful to make a comparison with the work of TK. The underlying assumption in TK is that throughout the evolution the axial length scale is asymptotically larger than the radial one so that their ratio is $1/\epsilon$ with $\epsilon \ll 1$ (the parameter ϵ is arbitrary and is not connected to scales given by linear stability for example). Next proceed as follows (details may be found in TK): expand quantities in power series of ϵ^2 which gives a leading-order solution of Laplace's equation independent of z; substitution of this solution into the kinematic and Bernoulli equations yields a coupled system of nonlinear PDE's written as

$$S_t + \tfrac{1}{2}SW_z + S_z W = 0, \tag{2.15}$$

$$W_t + WW_z = S_z/S^2, \tag{2.16}$$

where $S(t, z)$ is the scaled jet shape and $W(t, z) = \phi_z(t, z)$ with $\phi(t, z)$ the leading-order potential (W therefore is the axial velocity of the jet, to leading order). These equations are identical to those derived and used in TK if ϕ is adopted in favour of W. In accordance with (2.3*a–d*) we seek singular solutions (as $t \to t_s -$) of the form

$$S(t, z) = \tau^{\alpha} f_0(\xi), \quad W(t, z) = \tau^{\gamma_1} g(\xi), \quad z = \tau^{\beta}\xi,$$

which give the following scalings and scaling functions:

$$\alpha = 2 - 2\beta, \quad \gamma_1 = \beta - 1, \tag{2.17}$$

$$-(2-2\beta)f_0 + \beta\xi f_0' + \tfrac{1}{2}f_0 g' + g f_0' = 0, \quad (1-\beta)g + \beta\xi g' + gg' = f_0'/f_0^2. \tag{2.18a, b}$$

Equations (2.11) and (2.14) are seen to be identical to (2.18*a*, *b*) once the substitution $A' \to g$ is made and (2.14) is differentiated once. Numerical solutions of (2.18*a*) and (2.18*b*) have been given in TK (TK study dynamics just beyond pinching, but as a referee points out a simple transformation gives dynamics just before pinching and hence solutions of (2.11) and (2.14)) and so are omitted here. The asymptotic behaviour at infinity is easily found (see TK also) to be

$$f_0 \sim |\xi|^{2(1-\beta)/\beta}, \quad g \sim |\xi|^{-(1-\beta)/\beta}, \quad |\xi| \to \infty, \tag{2.19a, b}$$

while the outer solutions have the following asymptotic forms as $|z| \to 0$:

$$S(t, z) \sim |z|^{2(1-\beta)/\beta}, \quad W(t, z) \sim |z|^{-(1-\beta)/\beta}, \quad |z| \to 0.$$

In an attempt to verify the singular structures given by solutions of (2.18*a*, *b*) the one-dimensional system (2.15), (2.16) was solved numerically. Periodic boundary conditions are imposed in the axial direction and spectral methods are used to integrate the equations. It is found that solutions tend to terminate in infinite slope singularities

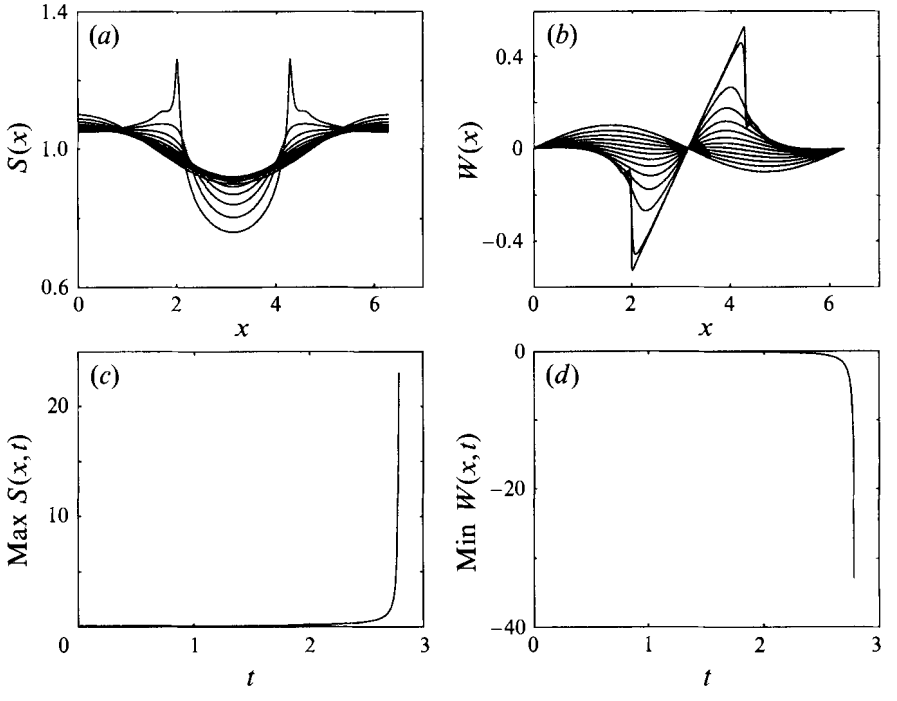

FIGURE 1. Numerical solutions of the inviscid one-dimensional model equations indicating infinite slope singularity after a finite time. The computation is stopped when the maximum of either $|S_x|$ or $|W_x|$ gets larger than 20. (*a*) Evolution of $S(x, t)$, (*b*) evolution of $W(x, t)$, (*c*) evolution of the maximum slope of $S(x, t)$, (*d*) evolution of the minimum slope of $W(x, t)$.

after a finite time for different initial conditions. Representative solutions are depicted in figure 1 (*a–d*). The initial conditions used utilize a symmetry of the equations, namely that if S and W are even and odd respectively at $t = 0$, then they remain so for subsequent times. In particular figure 1 was obtained for the following initial conditions:

$$S(z, t = 0) = 1 + 0.1\cos(z), \quad W(z, t = 0) = 0.1\sin(z).$$

The accuracy of the computation is monitored by noting that the integrals of S^2 and W are conserved quantities. Figure 1 (*c*, *d*) shows the time evolution of the maximum of S_x and the minimum of W_x. The numerical solutions suggest, therefore, that infinite slope singularities are encountered after a finite time and before the jet radius vanishes; it can be concluded, therefore, that from this class of numerical experiment, at least, we do not see any evidence of pinching solutions but instead see a violation of the slender-jet assumption. It is possible that pinching solutions can be achieved by changing the boundary conditions (for example removing fluid from the ends of the computational domain) but our interest is in a local breakup which is not sensitive to conditions far away from the pinch point. Since infinite slope singularities herald a violation of the model, no attempt has been made to analyse their local behaviour. We note also that numerical solutions on periodic domains of the viscous one-dimensional long-wave models do not violate the slender-jet ansatz used to derive them and instead produce pinching solutions consistent with the self-similar forms provided by the asymptotic theory (see Eggers 1993 and Papageorgiou 1995 for Navier–Stokes and Stokes flows respectively).

2.2. *General theory*, $\alpha = \beta$

Guided by the fact that numerical solutions of the initial value problem of the slender-jet model indicate that axial and radial scales do not remain disparate, we now consider pinching occurring on axial and radial length scales which are comparable. This amounts to taking $\alpha = \beta$ in the scalings (2.2*a–c*). The balance (2.10) still holds from the kinematic condition while a balance between surface tension and convection terms in the Bernoulli equation fixes the value of $\beta = \frac{2}{3}$ (this can also be seen from (2.13) by setting $\alpha = \beta$). The following scalings are found:

$$(r, z) = \tau^{2/3}(y, \xi), \quad S(t, z) = \tau^{2/3} f(\xi), \quad \phi(t, r, z) = \tau^{1/3}\chi(y, \xi). \tag{2.20a–c}$$

We note that the scaling functions $f(\xi)$ and $\chi(y, \xi)$ are now exact similarity solutions since all terms in the governing equations (2.1*a–c*) are of the same order as a pinch forms. The consequence of this is that the governing system in the similarity region is an elliptic partial differential one with a free nonlinear boundary which is to be determined. This system is

$$\chi_{yy} + \frac{1}{y}\chi_y + \chi_{\xi\xi} = 0; \tag{2.21a}$$

on $y = f(\xi)$

$$\chi_y = \tfrac{2}{3}(\xi f' - f) + f'\chi_\xi, \tag{2.21b}$$

$$\tfrac{1}{3}(2\xi\chi_\xi + 2f\chi_y - \chi) + \tfrac{1}{2}(\chi_y^2 + \chi_\xi^2) = -\left[\frac{1}{f} - f'' + \frac{(f')^2 f''}{1 + (f')^2}\right](1 + (f')^2)^{-1/2}. \tag{2.21c}$$

Equations (2.21*b*, *c*) are the boundary conditions at the free surface while regularity of solutions provides another condition at $y = 0$. In order to be able to obtain the similarity, field conditions at infinity need to be specified also. Solutions to (2.21*a–c*) have not been obtained yet; Keller & Miksis (1983) have solved the analogous two-dimensional problem and the system above is the axisymmetric extension to that. It would be interesting to see if solutions to the axisymmetric system support the wavy capillary ripples far away from the pinching region computed by Keller & Miksis. Such wavy behaviour away from the pinch has also been observed in the experiments of Peregrine *et al.* (1990) for axisymmetric jets.

3. Theory for highly viscous jets

In this section we consider the collapse of a viscous thread of fluid of undisturbed radius R under capillary instability. In numerous applications characteristic Reynolds numbers are small and the flow is governed by the Stokes equations. Such flows are driven by capillary forces which in turn provide a scale for the flow velocities. In non-dimensionalizing the equations, therefore, the following scales are used:

$$(r, z) = R(\bar{r}, \bar{z}), \quad (u, w) = \frac{\sigma}{\mu}(\bar{u}, \bar{w}), \quad p = \frac{\sigma}{R}\bar{p}, \quad t = \frac{\mu R}{\sigma}\bar{t},$$

where σ is the surface tension coefficient and μ the fluid viscosity. The non-dimensional equations and interfacial boundary conditions become (dropping the bars)

$$\nabla^2 u - \frac{1}{r^2}u = p_r, \quad \nabla^2 w = p_z, \quad \frac{1}{r}(ru)_r + w_z = 0, \tag{3.1a–c}$$

$$\nabla^2 \equiv \frac{\partial^2}{\partial r^2} + \frac{1}{r}\frac{\partial}{\partial r} + \frac{\partial^2}{\partial z^2}.$$

On $r = S(t,z)$ we have

$$(u_z + w_r)(1 - S_z^2) + 2u_r S_z - 2w_z S_z = 0, \tag{3.1d}$$

$$p - 2u_r - (-p + 2w_z) S_z^2 + 2(u_z + w_r) S_z = -\left(S_{zz} - \frac{1}{S}(1 + S_z^2)\right)(1 + S_z^2)^{-1/2}, \tag{3.1e}$$

$$u = S_t + wS_z. \tag{3.1f}$$

The interfacial conditions (3.1*d–f*) represent the tangential stress balance, normal stress balance and the kinematic condition respectively. An additional condition is regularity of the velocity field on the jet axis $r = 0$. The problem (3.1*a–f*) poses a formidable analytical task. Analytical studies are usually confined to linear stability and in the fully nonlinear regime the problem has been addressed numerically (see the Introduction). In order to draw up an analogy with the inviscid analysis of §2, we can introduce a streamfunction ψ defined by $u = -(1/r)\psi_z$, $w = (1/r)\psi_r$ so that the continuity equation (3.1*c*) is satisfied. Elimination of p between (3.1*a*, *b*) yields a single equation for ψ, namely

$$\mathrm{E}^4\psi = 0, \quad \mathrm{E}^2 \equiv \nabla^2 - \frac{2}{r}\frac{\partial}{\partial r}. \tag{3.2}$$

The flow field in the viscous case is governed by a fourth-order equation as opposed to the second-order Laplace equation for the potential in inviscid flows. As seen below the analysis of viscous jet pinching is slightly more involved. In what follows we choose to work with primitive variables rather than with the streamfunction ψ.

Following the ideas developed in §2, we look for singular terminal states of (3.1*a–f*) according to the ansatz

$$r = (t_s - t)^\alpha y, \quad z = (t_s - t)^\beta \xi, \quad S = (t_s - t)^\alpha f(\xi), \tag{3.3a–c}$$

$$w = (t_s - t)^\gamma W(t, y, \xi), \quad u = (t_s - t)^{\gamma + \alpha - \beta} U(t, y, \xi), \quad p = (t_s - t)^{-\alpha} P. \tag{3.3d–f}$$

The expression for u follows from the continuity equation (3.1*c*) once w is specified, and the scaling for the pressure p is a consequence of the normal stress balance equation (3.1*e*) since capillary instability drives the dynamics. Assuming a long-wave ansatz at pinching implies the inequality

$$\alpha > \beta. \tag{3.4}$$

Consideration of equation (3.1*b*) for w indicates that if a leading-order balance is made between the radial derivative terms of w and the pressure gradient term (this requires $\gamma = \alpha - \beta$), the following *leading-order* solution for W arises:

$$W = \tfrac{1}{4} y^2 P_\xi + A(\xi), \tag{3.5}$$

where $A(\xi)$ is an unknown function. An inconsistency appears now if (3.5) is substituted into the tangential stress balance equation (3.1*d*). The leading-order contribution to (3.1*d*) after substitution of the scalings (3.3) is simply $W_y = 0$ on $y = f(\xi)$. Application of this condition to the solution (3.5) found above implies that $P_\xi f(\xi) = 0$ leading to an inconsistent solution $P = \text{const}$. A consistent solution is constructed by expanding W (and therefore U) in appropriate powers of $(t_s - t)$ with the leading-order contribution of W being independent of y so that the tangential stress balance is satisfied identically to leading order. Another way to see that the leading-order solution for W is independent of y is from equation (3.2) for the streamfunction after making the transformations (3.3); in fact, these scalings indicate that the streamfunction has an expansion

$$\psi = \tau^\gamma(\psi_0 + \tau^{2\alpha - 2\beta}\psi_1 + O(\tau^{4\alpha - 4\beta}),$$

and the equation satisfied by ψ_0 is

$$\psi_{0yyyy} - \frac{2}{y}\psi_{0yyy} + \frac{3}{y^2}\psi_{0yy} - \frac{3}{y^3}\psi_{0y} = 0,$$

with solution $\psi_0 \equiv \psi_0(\xi)$ by demanding regularity at $y = 0$. The appropriate expansions for w and u become, then,

$$w = \tau^{\gamma}(W_0(\xi) + \tau^{2\alpha-2\beta}W_1 + \ldots), \tag{3.6a}$$

$$u = \tau^{\gamma+\alpha-\beta}(U_0(y,\xi) + \tau^{2\alpha-2\beta}U_1 + \ldots). \tag{3.6b}$$

In general an expansion for $f(\xi)$ is also needed but since higher-order terms are not required in the analysis that follows (and that of §4) we work with $f(\xi)$ where it should be understood to be a leading-order quantity. The solution for U_0 which is regular at $y = 0$ follows from (3.1c):

$$U_0 = -\tfrac{1}{2}yW_{0\xi}. \tag{3.7}$$

Next we obtain the solutions for W_1 and U_1. Using (3.3) and (3.6a) in equation (3.1b) gives

$$\tau^{\gamma-2\beta}\left(\frac{\partial^2}{\partial y^2} + \frac{1}{y}\frac{\partial}{\partial y}\right)(W_1) + \tau^{\gamma-2\beta}W_{0\xi\xi} + \ldots = \tau^{-\alpha-\beta}P_{\xi}. \tag{3.8}$$

Balance of the leading-order terms involving W_0, W_1 and P gives

$$\gamma = \beta - \alpha, \tag{3.9}$$

and a solution for W_1 follows by integration with respect to y since the pressure is independent of y by the normal stress balance (see comments below also):

$$W_1 = \tfrac{1}{4}y^2(P_{\xi} - W_{0\xi\xi}) + A(\xi), \tag{3.10}$$

where A is some function of ξ. Using (3.10) and (3.1c) gives

$$U_1 = -\tfrac{1}{16}y^3(P_{\xi\xi} - W_{0\xi\xi\xi}) + \tfrac{1}{2}yA_{\xi}. \tag{3.11}$$

Implicit in the solutions (3.10), (3.11) is the assumption that $P_y = 0$. Using the values (3.9) in the radial momentum equation (3.1a) gives, to leading order,

$$\left(\frac{\partial^2}{\partial y^2} + \frac{1}{y}\frac{\partial}{\partial y} - \frac{1}{y^2}\right)U_0 = P_y. \tag{3.12}$$

Now substitution of the solution (3.7) for U_0 into (3.12) shows that the left-hand side is zero and so

$$P_y = 0, \tag{3.13}$$

showing consistency of the expansion.

Next we consider the tangential stress balance. Using the values (3.9) gives the following equation to leading order:

$$U_{0\xi} + W_{1y} + 2U_{0y}f' - 2W_{0\xi}f' = 0 \quad \text{on} \quad y = f(\xi). \tag{3.14}$$

Each term in (3.14) is of order $\tau^{\gamma+\alpha-2\beta} = \tau^{-\beta}$. Use of solutions (3.7) and (3.10) in (3.14) gives an ordinary differential equation for $W_0(\xi)$:

$$(f^3W_0')' = \tfrac{1}{2}f^3P'. \tag{3.15a}$$

An expression for P in terms of W_0 is available from the normal stress balance equation. It is found that to leading order several terms in this equation are in balance

(and of order $\tau^{-\alpha}$ in fact, according to the previously found values (3.9)), the resulting equation being

$$P-2U_{0y}=\frac{1}{f} \quad \text{on} \quad y=f(\xi). \tag{3.15b}$$

Substitution of (3.15*b*) into (3.15*a*) allows one integration to yield

$$W_0'=-\frac{1}{3f}+\frac{k}{f^2}, \tag{3.16}$$

where k is a constant of integration. With W_0 known in terms of f, an equation for f arises from the kinematic condition (3.1*f*) and use of the ansatz (3.3) along with the appropriate derivative transformations (see §2 also). To leading order, therefore, the kinematic condition becomes

$$\tau^{\gamma+\alpha-\beta}(-\tfrac{1}{2}fW_0')=\tau^{\alpha-1}(-\alpha f+\beta\xi f')+\tau^{\gamma+\alpha-\beta}W_0f'. \tag{3.17}$$

Balancing terms and using (3.9) gives

$$\alpha=1, \quad \gamma=\beta-1. \tag{3.18}$$

The system of equations to solve consists of (3.16) and

$$(W_0+\beta\xi)f'+\left(-f-\frac{1}{6}+\frac{k}{2f}\right)=0. \tag{3.19}$$

A single equation for f can be obtained by elimination of W_0 to give

$$\left(f^2+\frac{f}{6}-\frac{k}{2}\right)f''+\left(-\tfrac{1}{3}+(\beta-1)f+\frac{k}{2f}\right)(f')^2=0. \tag{3.20}$$

Equations (3.16) and (3.19) or equivalently equation (3.20) have a two-parameter family of solutions analysed next.

3.1. *Analysis of the similarity equations*

To facilitate comparison with the Navier–Stokes theory of the following Section we begin with the third-order system rather than the integrated form (3.16). This system is

$$W_0''+2\frac{f'}{f}W_0'+\frac{1}{3}\frac{f'}{f^2}=0, \tag{3.21a}$$

$$(W_0+\beta\xi)f'-f(1-\tfrac{1}{2}W_0')=0. \tag{3.21b}$$

(These are equations (4.7) and (4.8) below at zero Reynolds number and $\beta=\frac{1}{2}$ (see §4)). The following form of (3.21*a*) is useful in understanding the behaviour at infinity and in particular the similarities between the asymptotic behaviour of the Stokes theory and the corresponding one for the Navier–Stokes flow. Equation (3.21*a*) is easily rewritten as

$$\frac{1}{f^2}\frac{\mathrm{d}}{\mathrm{d}\xi}\left(f^2W_0'+\tfrac{1}{3}f'\right)=0. \tag{3.21c}$$

The behaviour of solutions for large $|\xi|$ is considered first. It is easy to show from (3.21*a*, *b*) that far from the pinch point the asymptotic form of the scaling functions is

$$f(\xi)\sim|\xi|^{1/\beta}, \quad W_0\sim|\xi|^{-(1-\beta)/\beta}. \tag{3.22a, b}$$

Since $\beta < 1$, it is seen that W_0 decays to zero and $f(\xi)$ increases without bound. These asymptotic expressions provide the form of the solutions as viewed from outside the similarity region. In fact using (3.22) in the ansatz (3.3) and rewriting variables in terms of z we see that the time dependence drops out and

$$S \sim z^{1/\beta}, \quad w \sim z^{-(1-\beta)/\beta},$$

to leading order. In constructing acceptable scaling functions that match with the outer flow it is necessary to pick out those solutions of the nonlinear system which give f growing unbounded as in (3.22) as $|\xi| \to \infty$.

Corrections to (3.22) are obtained by the substitution of those forms into (3.21 *a*, *b*) and solution for a linearized correction at infinity. The following series involving two parameters, k_0 and k_1, has been found as $\xi \to \infty$:

$$f(\xi) = k_0 \xi^{1/\beta} + \frac{1}{3(1-\beta)} - \tfrac{1}{6} + \ldots, \tag{3.23a}$$

$$W_0(\xi) = \frac{\beta}{3(1-\beta)k_0} \xi^{-(1-\beta)/\beta} + k_1 \xi^{-(2-\beta)/\beta} + \ldots. \tag{3.23b}$$

We can conclude from (3.23 *a*, *b*) that since W_0 is bounded and decays to zero at infinity, there is a point where $\beta\xi + W_0$ vanishes. From (3.20*b*), then, regularity of f implies that at such a point, ξ_0 say, we impose

$$1 - \tfrac{1}{2} W_0'(\xi) = 0. \tag{3.24a}$$

The point ξ_0 is a removable singularity and must be treated separately in numerical work for instance, The transformations

$$f \to f, \quad g(\eta) = W_0 + \beta\xi_0, \quad \eta = \xi - \xi_0,$$

shift the position of the singularity to $\eta = 0$; the only change is that the asymptotic value of the transformed variable g far from the pinch point is no longer zero but $\beta\xi_0$ with ξ_0 arbitrary. The conditions on g at $\eta = 0$ become

$$g(0) = 0, \quad g'(0) = 2. \tag{3.24b, c}$$

In what follows we show how a closed-form solution an be obtained which satisfies the conditions at infinity. It is useful to consider the integrated form of the equations (after an integration of (3.21 *c*))

$$f' = \frac{1 - \frac{1}{2}g'}{g + \beta\eta} f, \quad g' = -\frac{1}{3f} + \frac{k}{f^2}, \tag{3.25a, b}$$

where k is a constant to be determined. A single equation for f follows after elimination of g to give

$$f'' = \frac{(f')^2}{f} \frac{(1-\beta)f^2 + \frac{1}{3}f - \frac{1}{2}k}{(f + (3+2\beta)/[12(1+\beta)])(f - [1/12(1+\beta)])}. \tag{3.26}$$

Smooth solutions of (3.26) can be found which are symmetric about $\eta = 0$ (see below). Using this symmetry the following local solutions arise in the vicinity of $\eta = 0$:

$$f(\eta) = f_0 + \eta^2 f_2 + \eta^4 f_4 + \ldots, \quad |\eta| \ll 1, \tag{3.27a}$$

$$g(\eta) = 2\eta + g_3 \eta^3 + \ldots, \quad |\eta| \ll 1. \tag{3.27b}$$

Substitution of these expressions into (3.25*a*, *b*) gives the following equations for the leading coefficients:

$$2f_0^2+\tfrac{1}{3}f_0-k=0, \tag{3.28a}$$

$$(\tfrac{1}{3}+4f_0)f_2+3f_0^2g_3=0, \quad 2(\beta+2)f_2+\tfrac{3}{2}f_0g_3=0. \tag{3.28b, c}$$

The simultaneous system (3.28*b*) has a non-trivial solution if the determinant of coefficients vanishes, a condition that yields a value for f_0, and which in turn yields the value of k from (3.28*a*), both in terms of β:

$$f_0=\frac{1}{12(1+\beta)}, \quad k=\frac{3+2\beta}{72(1+\beta)^2}. \tag{3.29}$$

The remaining coefficients in (3.27*a*, *b*) are expressible in terms of a single arbitrary parameter, f_2 say.

Next we construct an implicit form for the solution $f(\xi)$. Equation (3.26) can be integrated once by separating variables and splitting the right-hand side into partial fractions to give the implicit form

$$\int_{1/12(1+\beta)}^{f}\frac{(f+[(3+2\beta)/12(1+\beta)])^{(2\beta+1)/2}}{f(f-1/12(1+\beta))^{1/2}}\mathrm{d}f=A\eta, \tag{3.30}$$

where A is a constant to be determined. The solution (3.29) has been given for positive η and can be extended to negative η by symmetry (f being symmetric with respect to η). One way to see this explicitly, is to make the substitution

$$f=\frac{1}{12(1+\beta)}\cosh^2(\theta),$$

so that $\theta=\pm\cosh^{-1}(12(1+\beta)f)^{1/2}$. The solution becomes, then,

$$\frac{1}{(12(1+\beta))^{\beta}}\int_0^{\theta}\frac{(\cosh^2\theta+3+2\beta)^{\beta+1/2}}{\cosh\theta}\mathrm{d}\theta=A\eta, \quad \eta>0, \tag{3.31a}$$

$$\frac{1}{(12(1+\beta))^{\beta}}\int_0^{\theta}\frac{(\cosh^2\theta+3+2\beta)^{\beta+1/2}}{\cosh\theta}\mathrm{d}\theta=-A\eta, \quad \eta<0. \tag{3.31b}$$

The constant A can be expressed in terms of the parameter f_2 introduced in (3.27*a*) above, by writing (3.31) for small η; this gives

$$A=\frac{24}{(1+\beta)}\left(\frac{2+\beta}{6(1+\beta)}\right)^{\beta+1/2}f_2^{1/2}.$$

With $f(\eta)$ known, the variation of g with η is obtained by integration of (3.25*a*) and yields

$$g(\eta)=\int_{-\infty}^{\eta}\left(-\frac{1}{3f}+\frac{k}{f^2}\right)\mathrm{d}\eta+\beta\xi_0, \tag{3.32}$$

with k given by (3.29) and ξ_0 arbitrary. The constants f_2 and ξ_0 are the parameters describing the two-parameter family of solutions for different values of β. Since $g(\eta)$ in (3.32) satisfies the conditions $g(\pm\infty)=\beta\xi_0$ the value of k (and hence β) is fixed from (3.32) to be

$$k=\frac{1}{3}\int_0^{\infty}f^{-1}\mathrm{d}\eta\Big/\int_0^{\infty}f^{-2}\mathrm{d}\eta. \tag{3.33}$$

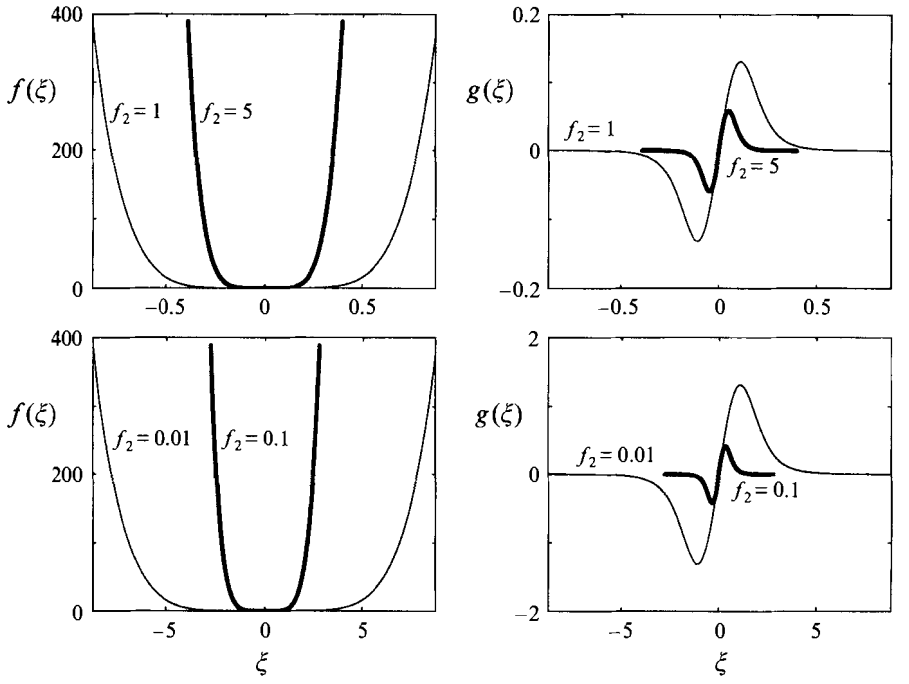

FIGURE 2. Stokes jet similarity solutions. The scaling functions $f(\xi)$ and $g(\xi)$ for different values of the scaling constant f_2 shown on the figure.

It has been confirmed numerically that the ratio of the integrals in (3.33) is independent of f_2 as expected from the expression (3.29) for k. Equation (3.33), then, is an eigenrelation of the form $\mathscr{F}(\beta) = 0$ which must be solved numerically. Before presenting numerical solutions, it is interesting to consider the limiting case $\beta = \frac{1}{2}$; as shown in the following Section which treats the Navier–Stokes flow, the Stokes flow is valid as long as $\beta < \frac{1}{2}$. With $\beta = \frac{1}{2}$ the integrals above can be carried out to give the following implicit solution for $f(\eta)$:

$$2(f-\tfrac{1}{18})^{1/2} + \frac{2\sqrt{2}}{3}\tan^{-1}(3\sqrt{2}(f-\tfrac{1}{18})^{1/2}) = A\eta, \tag{3.34}$$

with a symmetric expression valid for $\eta < 0$ and A as above but evaluated at $\beta = \frac{1}{2}$.

The numerical work has been carried out using (3.30) or (3.31) to determine $f(\xi)$ and (3.32) to obtain $g(\xi)$. The role of the parameter f_2 is simply a rescaling of the solutions by a multiplicative factor and does not affect the admissible unique value of β which is to be determined. Equation (3.30) is integrated by quadratures to yield the value of η at an interfacial amplitude f. It was found useful to remove the singularity by an integration by parts before the numerical implementation; more grid points (in f) are required near the minimum to maintain overall accuracy. The same procedure with (3.31) is preferable since the integrand is free of singularities. Given a value of β, then, the solution $f(\eta)$ is obtained over a large enough range. Equation (3.33) is used in an iteration scheme to compute the value of β. These computations give a value $\beta = 0.175$ correct to three decimal places. The scaling functions are unique to within a scaling factor and representative solutions are given in figure 2.

4. Pinching solutions of the Navier–Stokes equations

In this Section we consider the range of validity of the pinching solutions given previously according to the Stokes equations. The Stokes approximation is valid as long as the convective unsteady terms in the Navier–Stokes equations are negligible. In view of the non-dimensionalization in the beginning of §3, the Navier–Stokes equations read

$$Re(u_t + uu_r + uw_z) = -p_r + \nabla^2 u - \frac{u}{r^2}, \tag{4.1a}$$

$$Re(w_t + uw_r + ww_z) = -p_z + \nabla^2 w, \tag{4.1b}$$

while the continuity equation is (3.1*c*). The Reynolds number appearing above is $Re = \sigma\rho R/\mu^2$, also known as the capillary number in the literature, and measures the ratio between surface tension and viscous forces. In the Stokes equations (3.1*a*, *b*) the left-hand sides of (4.1*a*, *b*) above are dropped. The validity of our highly viscous solutions can be seen from the form of the expansion (3.6*a*) for instance, where the leading-order contribution to the axial velocity of $O(\tau^{\beta-1})$ and so blows up as $\tau \to 0$. The theory of §3 uses information from the first two leading-order terms of w and the leading order in u (equations (3.6*a*, *b*)) and p. For clarity let us rewrite the ansatz in terms of the single parameter β:

$$w = \tau^{\beta-1} W_0(\xi) + \tau^{1-\beta} W_1 + \ldots, \quad u = U_0(y,\xi) + \tau^{2-2\beta} U_1 + \ldots, \tag{4.2a, b}$$

with W_i, U_i, $i = 0, 1$ known. Consider next the substitution of (4.2*a*, *b*) into (4.1*a*, *b*). The first stage where the theory of §3 is violated arises when the largest terms on the left of (4.1*a*, *b*) are of the same order as the smallest terms retained on the right of the Stokes theory. The largest term on the right of (4.1*a*) needed in the Stokes theory have $O(\tau^{-2})$ (see (3.12)), while the largest terms on the left have $O(\tau^{1-2\beta})$ (the unsteady term) and $O(\tau^{-1})$ (convective terms); the unsteady term becomes comparable to the terms retained on the right when $\beta = \frac{3}{2}$, which is outside the range of slender-jet ansatz, $\beta < 1$ and so is dropped (see comments below also). The radial momentum equation (4.1*a*), therefore, is accurately described by the asymptotic solutions found in §3, as limiting solutions of the Navier–Stokes equations as $\tau \to 0$.

The axial momentum equation (4.1*b*) is more important in this limit. Carrying out a similar order-of-magnitude analysis we see that the smallest diffusive and pressure terms required in the Stokes theory have $O(\tau^{-1-\beta})$ (see derivation of (3.8)). The largest terms appearing on the left include all three terms and have $O(\tau^{\beta-2})$. The Stokes theory of §3 is asymptotically consistent, then, as long as

$$\tau^{\beta-2} \ll \tau^{-1-\beta}, \quad \tau \to 0,$$

which imply the inequality

$$\beta < \tfrac{1}{2}.$$

As shown below, the leading-order balances in the tangential and normal stress balance equations and the kinematic condition are as before. We note that this still describes slender jets since $\beta < 1$ also. The limiting case is $\beta = \frac{1}{2}$, when the convective terms of the axial momentum Navier–Stokes equation enter.

With $\beta = \frac{1}{2}$, the following expansions are used:

$$w = \tau^{-1/2} W_0(\xi) + \tau^{1/2} W_1(y,\xi) + \ldots, \quad u = U_0(y,\xi) + \tau U_1(y,\xi) + \ldots, \tag{4.3a, b}$$

$$S(t,z) = \tau f(\xi), \quad p = \tau^{-1} P(y,\xi) + \ldots, \quad r = \tau y, \quad z = \tau^{1/2}\xi. \tag{4.3c–f}$$

The functions W_i, U_i and P are to be determined and should not be confused with those of §3. The main difference between these solutions and those of §3 lies in the determination of the function $W_1(y,\xi)$. Substitution of (4.3*a*, *c*) into (4.1*a*, *b*) gives

$$P_y = 0, \tag{4.4}$$

$$Re(\tfrac{1}{2}(W_0+\xi W_0')+W_0 W_0') = -P' + W_{1yy} + \frac{1}{y} W_{1y}, \tag{4.5}$$

where primes denote ξ-deriatives and (4.4) has been used to infer that P is a function of ξ alone. The solution of (4.5) which is regular at $y = 0$ is

$$W_1(y,\xi) = \tfrac{1}{4}y^2 \frac{\mathrm{d}}{\mathrm{d}\xi}(P - W_0' + \tfrac{1}{2}Re(\xi W_0 + W_0^2)) + A(\xi), \tag{4.6}$$

with $A(\xi)$ an arbitrary function of ξ. A solution for U_1 then follows from the continuity equation but is omitted here since it is not needed in the final result. The leading-order contributions of the tangential stress balance, the normal stress balance and the kinematic condition are exactly equations (3.15*a*, *b*) and (3.17) respectively with $\beta = \frac{1}{2}$. This follows easily from the analysis of §3. The influence of the convective terms is felt through the coupling provided by the tangential stress balance and the radial derivative of the axial velocity.

The required equations, then, arise from the tangential stress balance and the kinematic condition evaluated at $y = f$. Using the solution (4.6) in the latter along with the leading-order solutions found in §3, gives the following system of equations:

$$3W_0'' + \frac{f'}{f^2} + 6\frac{W_0' f'}{f} = Re(\tfrac{1}{2}(W_0+\xi W_0')+W_0 W_0'), \tag{4.7}$$

$$(W_0 + \tfrac{1}{2}\xi)f' - f(1 - \tfrac{1}{2}W_0') = 0. \tag{4.8}$$

Note that the presence of terms involving the Reynolds number in (4.7) does not enable integration of (4.7). In the limit $Re = 0$ equation (4.7) reduces to (3.16) after one integration (the limit is a regular one since it does not involve a vanishing second derivative). We also note that equations (4.7) and (4.8) have also been derived by Eggers & Dupont (1993) and Papageorgiou (1994) who employ a slender-jet approximation first to reduce the Navier–Stokes equations and boundary conditions to a coupled set of nonlinear partial differential equations involving t and z alone. As shown by Eggers & Dupont (1993) and Papageorgiou (1994) the one-dimensional model equations admit pinching solutions with exactly the scalings found here, and with the scaling functions satisfying (4.7) and (4.8) exactly.

The behaviour of the solutions far from the pinch point is important as it provides the correct behaviour for the outer solution. For large $|\xi|$, then, the main balances in (4.7) and (4.8) are

$$W_0 + \xi W_0' \sim 0, \quad \tfrac{1}{2}\xi f' - f \sim 0,$$

respectively, leading to the asymptotic forms

$$W_0(\xi) \sim \xi^{-1}, \quad f(\xi) \sim \xi^2 \quad \text{as} \quad |\xi| \to \infty. \tag{4.9a, b}$$

Rewriting these conditions in terms of the outer variables (4.3*d*) gives the following asymptotic behaviour for the outer solutions as $z \to 0$:

$$w \sim z^{-1}, \quad S \sim z^2 \quad \text{as} \quad |z| \to 0. \tag{4.10a, b}$$

In fact the asymptotic behaviour for large $|\xi|$ can be determined in terms of two parameters as follows. From (4.9*a*, *b*) we write

$$W_0 \sim c_0 \xi^{-1} + \tilde{W}_0, \quad f \sim c_1 \xi^2 + \tilde{f} \quad \text{as} \quad |\xi| \to \infty,$$

where tilde quantities are small compared to the leading terms. Substitution of these expressions into (4.7) and (4.8) and linearization with respect to $\tilde{W}_0$ and $\tilde{f}$ leads to the following leading-order balances:

$$\tfrac{1}{2} Re(\tilde{W}_0 + \xi \tilde{W}_0') = \left(Re\, c_0^2 + \frac{2}{c_1} - 6c_0 \right) \xi^{-3},$$

$$\tfrac{1}{2} \xi \tilde{f}' - \tilde{f} = -\tfrac{3}{2} c_0 c_1.$$

The particular solutions of these equations give the corrections $\tilde{W}_0$ and $\tilde{f}$, and the process can be repeated to obtain higher-order corrections all in terms of the two parameters c_0 and c_1. The first two terms in the series are

$$W_0(\xi) = c_0 \xi^{-1} + \frac{1}{Re} \left(6c_0 - \frac{2}{c_1} - Re\, c_0^2 \right) \xi^{-3} + \ldots, \quad |\xi| \to \infty, \tag{4.11a}$$

$$f(\xi) = c_1 \xi^2 + \tfrac{3}{2} c_0 c_1 + \ldots, \quad |\xi| \to \infty. \tag{4.11b}$$

It is interesting to compare (4.11*a*, *b*) with the corresponding Stokes flow equations (3.21) as $Re \to 0$. In this limit the second term in (4.11*a*) remains regular if

$$c_0 = 1/(3c_1),$$

and making the correspondence $c_1 \to k_0$ between (4.11) and (3.23*a*, *b*) together with $\beta = \frac{1}{2}$ shows that the two series are in agreement except for the second-order correction for W_0.

It can be seen from (4.11*a*, *b*) that two parameters appear at infinity. The solutions to (4.7) and (4.8) are described by a three-parameter family and the remaining condition is found from the regularity of f over its domain. As shown in §3.1 the appropriate conditions are

$$W_0(\xi_0) + \tfrac{1}{2}\xi_0 = 0, \quad 1 - \tfrac{1}{2} W_0'(\xi_0) = 0,$$

and a local solution near $\xi = \xi_0$ has been found in terms of the two parameters ξ_0 and f_0:

$$f(\xi) = f_0 + \frac{f_0^2 Re\, \xi_0}{4(3f_0 - 1)} (\xi - \xi_0) + f_0^2 Re \times \frac{-48 + 288 f_0 - 432 f_0^2 - f_0 Re\, \xi_0^2 + 9 f_0^2 Re\, \xi_0^2}{16(3f_0 - 1)^2 (18 f_0 - 1)} (\xi - \xi_0)^2 + \ldots, \tag{4.12a}$$

$$W_0(\xi) = -\tfrac{1}{2}\xi_0 + 2(\xi - \xi_0) - \frac{5 f_0 Re\, \xi_0}{8(3f_0 - 1)} (\xi - \xi_0)^2 + \ldots. \tag{4.12b}$$

Equations (4.11*a*, *b*) and (4.12*a*, *b*) clearly show that we are dealing with a three-parameter family of solutions. For instance, if the asymptotic constants c_0 and c_1 are known (note that different values obtain at $\pm\infty$ even though we use the same notation), then a shooting method must be employed in a numerical integration from the neighbourhood of the removable singularity out to infinity to yield a unique set of

scaling functions. Here we are interested in the dynamics beyond the breakup (see §5) which require the constants c_1 and c_2. Numerical solutions of the system (4.7), (4.8) have been obtained by Eggers (1993, 1995) and some of those results are used below.

5. The dynamics beyond pinching for Stokes and Navier–Stokes jets

In this section we follow the ideas of Taylor (1959), Keller (1983) and TK to follow the evolution of the jet beyond pinching by a simple analytical model that captures the main features of the dynamics. The theory will be presented for viscous jets and inviscid analyses can be found in TK and Keller *et al.* (1995). The slender-jet ansatz is valid up to the point of breakup and the solutions given in the previous Sections describe the local flow up to that time. Just beyond breakup the jet separates and the two ends accelerate away from the breaking point. The models proposed by the authors cited above, and which are in line with experimental observations, assume that the jet ends at some point, $X(t)$ say, and a blob of fluid of mass $M(t)$ is attached to this end. Mass and momentum balance arguments provide evaluation equations for $M(t)$ and $X(t)$ which need to be solved subject to initial conditions which coincide with the solutions just before breakup. There is a difference between the viscous and the inviscid theory, in that the exponent β is not fixed for the latter and so some jet shape must be taken in order to fix it; TK carry out the analysis for several different values of β which probably correspond to self-similar solutions evolving from different initial and boundary conditions. For the viscous theory presented earlier the values of β are fixed and so are the scaling functions (see later also). The model is completed by using information in the equations for $M(t)$ and $X(t)$ about the flow field as solved by the self-similar slender-jet theory.

The first equation comes from a mass balance of the blob. The following dimensional variables are used: $M(t)$ is the blob mass, $X(t)$ is the axial distance from the breaking point where the blob is attached to the slender jet, $S(X, t)$ is the jet radius there and W is the axial velocity. The mass balance is

$$\frac{\mathrm{d}M}{\mathrm{d}t} = \pi\rho S^2\left(\frac{\mathrm{d}X}{\mathrm{d}t} - W\right). \tag{5.1}$$

The second equation comes from a balance of momentum. Again we carry this out using dimensional variables. The forces acting on the blob at $X(t)$ have two contributors: a viscous stress force and a surface tension pull. If we denote the axial component of the viscous stress by T_{zz} and the radial component by T_{rr}, then the total force on the cross-section at $X(t)$ is

$$F = \pi S^2(T_{zz} - p) + 2\pi\sigma S,$$

and using the normal stress balance equation for slender jets,

$$p = T_{rr} + \sigma/S,$$

yields

$$F = \pi S^2(T_{11} - T_{rr}) + \pi\sigma S = 3\pi\mu S^2 W_z + \pi\sigma S, \tag{5.2}$$

with the final expression following from the slender-jet geometry. Stokes jets do not possess inertia and so the force in (5.2) is constant at all cross-sections; instead of the momentum balance given below then, in the analysis of Stokes jets the equation to be used along with (5.1) is

$$\frac{\partial}{\partial z}(3\pi\mu S^2 W_z + \pi\sigma S) = 0. \tag{5.3}$$

Introduction of the similarity variables (3.3) into (5.3) gives equation (3.16) as expected. This observation was used by Renardy (1994) in his analysis of slender Newtonian and viscoelastic jets with no inertia (see the Introduction) and our results are consistent. For jets with inertia a balance of momentum yields

$$\frac{\mathrm{d}}{\mathrm{d}t}\left(M\frac{\mathrm{d}X}{\mathrm{d}t}\right) = 3\pi\mu S^2 W_z + \pi S + W\frac{\mathrm{d}M}{\mathrm{d}t}. \tag{5.4}$$

When equations (5.1) and (5.4) are non-dimensionalized using the capillary scales given at the beginning of §3, we find

$$\frac{\mathrm{d}M}{\mathrm{d}t} = \pi S^2\left(\frac{\mathrm{d}X}{\mathrm{d}t} - W\right), \tag{5.5a}$$

$$Re\frac{\mathrm{d}}{\mathrm{d}t}\left(M\frac{\mathrm{d}X}{\mathrm{d}t}\right) = 3\pi S^2 W_z + \pi S + Re\, W\frac{\mathrm{d}M}{\mathrm{d}t}, \tag{5.5b}$$

where the same symbols have been used to denote non-dimensional quantities. The inviscid equations of TK are recovered by dropping the viscous stress term $S^2 W_z$ from (5.4) and scaling the capillary number out of the problem. In what follows we consider the dynamics beyond pinching for Stokes and Navier–Stokes jets.

5.1. *Stokes jets*

Suppose the jet pinches at $t = 0$ at some axial position. The local structure of the solution as this time is approached from below has been given in §4. The flow field as viewed from the outer region is obtained from the large-ξ asymptotics of (3.23). The constant k_0 is easily determined by writing (3.32) for large θ and the result is

$$S(z,0) = c_1 z^{1/\beta}, \quad W(z,0) = c_2 z^{-(1-\beta)/\beta}, \tag{5.6a, b}$$

$$c_1 = \left[\frac{48\beta}{1+\beta}\left(\frac{2+\beta}{6(1+\beta)}\right)^{\beta+1/2}\right]^{1/\beta} f_2^{1/(2\beta)}, \quad c_2 = \frac{\beta}{3(1-\beta)c_1}. \tag{5.6c, d}$$

Away from the fluid blob, i.e. for $z > X(t)$, a solution can be sought of the form (3.3) which for $0 < t \ll 1$ is of the form

$$r = ty, \quad z = t^\beta \xi, \quad S(t,z) = tf(\xi),$$
$$W(t,r,z) = t^{\beta-1}W_0(\xi) + \ldots, \quad u = -\tfrac{1}{2}yW_{0\xi} + \ldots, \quad p = t^{-1}P(\xi) + \ldots. \tag{5.7}$$

The analysis presented in §4 leading to the system of similarity equations (3.16) and (3.19) is slightly modified by the fact that beyond pinching we have

$$\frac{\partial}{\partial t} \to \frac{\partial}{\partial t} - \frac{\beta\xi}{t}\frac{\partial}{\partial \xi} - \frac{y}{t}\frac{\partial}{\partial y},$$

instead of (2.3*e–g*), and consequently the system of similarity equations becomes

$$W_0' = -\frac{1}{3f} + \frac{k}{f^2}, \tag{5.8a}$$

$$(W_0 - \beta\xi)f' + \left(f - \frac{1}{6} + \frac{k}{2f}\right) = 0. \tag{5.8b}$$

The value of k in (5.8*b*) has is given in terms of $\beta = 0.175$ by (3.29). The objective is to incorporate information from solutions of (5.8*a*, *b*) into the mass balance equation

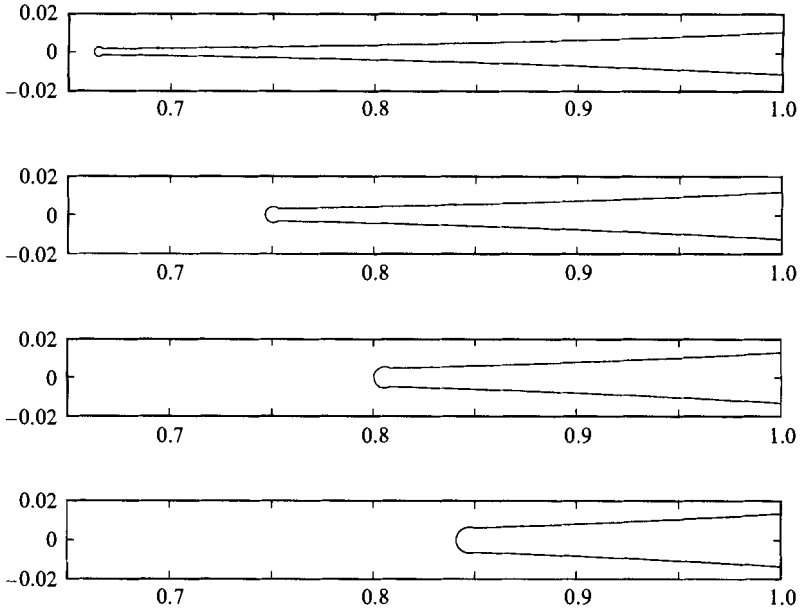

FIGURE 3. Stokes jet. Dynamics just beyond breakup – composite mass balance equation with similarity forms. Jet shape shown at successive time intervals of 0.0001. The motion is from left to right.

(5.5*a*). The Stokes flow equivalent of (5.5*b*) is (5.8*a*) in the similarity region at least. Numerical solutions of (5.8*a*, *b*) are required which begin at $+\infty$ and extend to the point where the fluid blob begins. As was pointed out by TK, even though the solutions may be continued to $-\infty$ they are only valid up to the point where the fluid blob begins since the blob dynamics are incompatible with the ansatz (5.7). The numerical strategy, then, is to prescribe initial conditions at infinity in terms of the asymptotic behaviour of the solutions there by using (5.6) to obtain $f(\xi) \sim c_1 \xi^{1/\beta}$, $W_0(\xi) \sim c_2 \xi^{-(1-\beta)/\beta}$ as $\xi \to \infty$, noting that the constants c_1 and c_2 are known numbers once f_2 is prescribed.

Finally a solution of (5.5*a*) is required. The appropriate solution has the similarity form

$$X(t) = X_0 t^{\beta}, \quad S(t, X_0) = tf(X_0), \quad W(t, X_0) = t^{\beta-1} W_0(X_0),$$

from which it follows that

$$M(t) = \frac{f^2(X_0)[\beta X_0 - W_0(X_0)]}{\beta+2} t^{\beta+2}. \tag{5.9}$$

for a given value of X_0 (which must satisfy the condition $\beta X_0 - W_0(X_0) > 0$ for the mass to be positive), equation (5.9) gives the mass of the blob at later times. In figure 3 we present a schematic of the evolution of the break in the jet according to equations (5.8*a*, *b*) and (5.9). The figure is produced as follows. Equations (5.8*a*, *b*) are solved numerically starting from a value ξ_∞ and integrating into the point $\xi = X_0$. This provides the scaling functions $W_0(\xi)$ and $f(\xi)$ for $X_0 \leqslant \xi \leqslant \xi_\infty$. The mass $M(t)$ is then computed from (5.9) at four different instants from which a radius for the blob to be attached at $z = t^{\beta} X_0$ is found (we assume that the fluid blob is a section of a sphere). The motion is from left to right and is shown at equal time intervals of 0.001. Owing to the symmetry of the solutions the motion to the left of the break is similar. The value

of X_0 comes from the solution of the time-dependent breakup and depends on initial conditions (for a solution of the time-dependent problem for slender jets, see Papageorgiou 1995).

5.2. *Navier–Stokes jets*

For Navier–Stokes jets the equations that give the scaling functions beyond pinching are

$$3W_0''+\frac{f'}{f^2}+6\frac{W_0'f'}{f} = Re(-\tfrac{1}{2}(W_0+\xi W_0')+W_0W_0'), \tag{5.10a}$$

$$(W_0-\tfrac{1}{2}\xi)f'+f(1+\tfrac{1}{2}W_0') = 0. \tag{5.10b}$$

Note that Re can be scaled out of the equations by the transformations

$$f\to f, \quad W_0\to Re^{-1/2}W_0, \quad \xi\to Re^{-1/2}\xi.$$

In what follows $Re = 1$ in all computations. The scaling functions just before pinching given by (4.7) and (4.8) have been obtained numerically by Eggers (1993, 1995). In particular he shows that these are universal and so the behaviour at infinity (equivalently the behaviour of the outer solution as $|z|\to 0$) is fixed as follows:

$$f(\xi)\sim b_1^{\pm}\xi^2, \quad W_0(\xi)\sim b_2^{\pm}\xi^{-1}, \tag{5.11a, b}$$

where the constants are

$$b_1^+ = 4.635, \quad b_1^- = 6.074\times 10^{-4}, \quad b_2^+ = 0.0723, \quad b_2^- = 57.043.$$

Using (5.11) in (5.10a, b) enables determination of unique solutions beyond pinching which are valid away from the break point at least (theoretically they are valid in regions where the jet is slender). Solutions of the mass and momentum balance equations (5.5a, b) are required in order to complete the picture. The following solution is valid for small t (see above and TK):

$$X(t) = X_0t^{1/2}, \quad S(t,X_0) = tf(X_0), \quad W(t,X_0) = t^{-1/2}W_0(X_0).$$

Substitution into (5.5a, b) yields an expression for the mass as well as a relation that determines the constant X_0. These are

$$M(t) = \tfrac{2}{5}\pi f^2(X_0)(\tfrac{1}{2}X_0-W_0(X_0)), \tag{5.12}$$

$$(\tfrac{2}{5}X_0-W_0(X_0))(\tfrac{1}{2}X_0-W_0(X_0))f(X_0)-3f(X_0)W_0'(X_0) = 1. \tag{5.13}$$

The constant X_0 was determined numerically from (5.13) by integration of (5.10a, b) starting with the unique asymptotic forms (5.11) and integrating inwards to the point where (5.13) is satisfied. The computed value was obtained by refining the grid as well as increasing the value of ξ_∞ until there is no change in the X_0 found, which was computed correct to two decimal places to be $X_0 = 0.91$. A picture of the dynamics to the right of the pinch point is given in figure 4 which was produced by the methods described earlier. The dynamics to the left of the pinch point are different and are easily computed by use of the asymptotic forms (5.11) at $\xi = \xi_{-\infty}$ and integration to increasing axial positions to determine X_0 and hence a hybrid solution analogous to that of figure 4. The important difference between the breakup of Navier–Stokes and Stokes jets and in particular their dynamics beyond pinching, within the context of the present theory, is that the former provide universal local solutions which are independent of initial conditions; Stokes jets, however, contain an arbitrary constant (the value of X_0) due to the absence of inertial terms. We note that different initial configurations will affect both the point where the pinch occurs and the time when it happens. The theory presented here describes what happens near this space–time singularity.

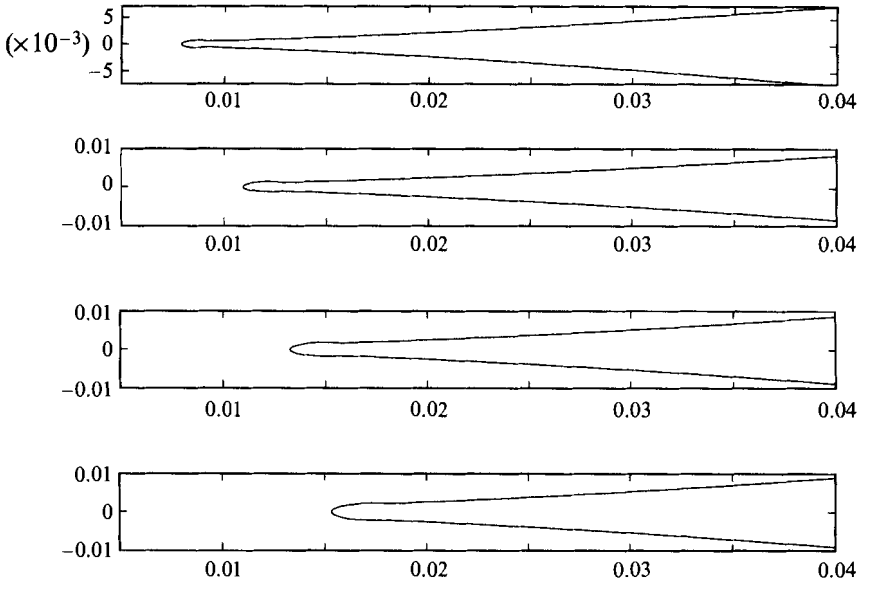

FIGURE 4. As figure 3 but for a Navier–Stokes jet.

6. Conclusions and discussion

A formal theory has been developed to describe the breakup process of viscous or inviscid jets in air. The similarity solutions obtained here constitute inner solutions in the vicinity of regions where the jet radius is going to zero which, when matched with outer solutions of the Euler, Stokes or Navier–Stokes equations respectively, provide a global description of the breakup phenomenon. In general the outer solutions are fully nonlinear and must be computed numerically. In numerical calculations of jet breakup it is important to have a rational way of continuing the computations beyond the change in topology necessitated by the physics and the similarity solutions presented here may provide such a possibility.

Past investigators have used one-dimensional long-wave model equations to describe the nonlinear evolution of jets (TK; Eggers & Dupont 1994; Eggers 1993, 1995; Renardy 1994; Papageorgiou 1995). Even though such approaches are based on the introduction of an arbitrarily long axial length scale they do provide information near pinching singularities if the latter are consistent with the underlying long-wave ansatz. The arbitrariness of the long axial length scale from the outset of the jet evolution is seen to be at variance with the order-one length scale predicted by linear theory since the wavelength of a maximally growing wave is independent of the surface tension and is a multiple of the undisturbed jet radius. The approach presented in this article is related but different in that it constructs asymptotically self-similar solutions directly from the full system of equations (Euler, Stokes or Navier–Stokes); in situations where the axial length scale is asymptotically larger than the radial one, complete agreement with singular solutions of one-dimensional model equations is found, as long as the evolution of the one-dimensional models preserve slenderness (see §2 also).

It has also been shown how the similarity solutions may be used to continue the flow beyond pinching. This is done by an overall mass and momentum balance in the neighbourhood of the receding jet end which use information from the similarity solutions away from the end points using the ideas first developed by Keller (1983) and TK for inviscid jets.

Finally we compare the theory for Stokes and Navier–Stokes jets. The values of the exponent β are found to be different; the reason for this is that the unsteady and convective terms in the axial momentum Navier–Stokes balance enter to fix $\beta = \frac{1}{2}$ then. Stokes solutions for $\beta = \frac{1}{2}$ can be formally written down (see (3.34)) but these are not strictly correct since the inertial and unsteady terms ignored are of the same order of magnitude as the terms retained as long as Re is of order one. Mathematically, the problem is fixed by letting Re tend to zero like some power of τ so that the inertial and unsteady terms drop out of the problem. The Stokes jet solution is then given by (3.33).

In the Stokes jet theory the constant of integration k in equation (3.25*b*) has a physical interpretation which follows from the fact that Stokes flows are inertialess (see Renardy 1994). The force acting on a cross-section of the Stokes jet is given by (5.2) and its slender (long-wave) equivalent. This force is constant since the flow does not possess inertia, which leads to condition (5.3). Integration with respect to z gives (in non-dimensional form)

$$3S^2W_z + S = K(t), \tag{6.1}$$

with $K(t)$ some function of time. As the pinch forms we write (6.1) in terms of the similarity variables introduced in §3; it is crucial, therefore, to have $K(t) = \tau k$ as $\tau \to 0$ in order to get equation (3.25*b*). If the force is locally smaller than $O(\tau)$ the alternative equation is

$$g' = -1/(3f),$$

and a local analysis as in §3 produces negative values of f_0 (see (3.2*a*)) which are not acceptable. It has been confirmed by numerical solution of the initial boundary problem for the one-dimensional model equations for Stokes jets (see Papageorgiou 1995), that $K(t) \sim \tau k$ as $\tau \to 0+$ for different initial conditions which produce pinching.

This research was supported by the National Science Foundation (DMS 9-9-0070) and by the Air Force Office for Scientific Research (grant No. F49620-94-1-0242). Additional support was provided by the National Aeronautics and Space Administration under NASA Contract Nos. NAS1-19480 and NAS1-18605 while the author was in Residence at the Institute for Computer Applications in Science and Engineering (ICASE), NASA Langley Research Center, Hampton, VA 23681-0001.

I would like to thank Professor Michael Renardy for numerous stimulating discussions concerning the analysis of jet breakup. I would also like to thank Jens Eggers for preprints of his work. Many constructive comments, suggestions and criticisms of the referees regarding earlier versions of the article are gratefully acknowledged. A referee is also thanked for bringing to my attention the recent work of Keller, King and Ting.

REFERENCES

BOGY, D. B. 1979 Drop formation in a circular liquid jet. *Ann. Rev. Fluid Mech.* **11**, 207–228.

CHANDRASEKHAR, S. 1961 *Hydrodynamic and Hydromagnetic Stability*. Clarendon Press.

CHAUDHARY, K. C. & MAXWORTHY, T. 1980*a* The nonlinear capillary instability of a liquid jet. Part 2. Experiments on jet behaviour before droplet formation. *J. Fluid Mech.* **96**, 275–286.

CHAUDHARY, K. C. & MAXWORTHY, T. 1980*b* The nonlinear capillary instability of a liquid jet. Part 3. Experiments on satellite drop formation and control. *J. Fluid Mech.* **96**, 287–297.

CHAUDHARY, K. C. & REDEKOPP, L. G. 1980 The nonlinear capillary instability of a liquid jet. Part 1. Theory. *J. Fluid Mech.* **96**, 257–274.

DONNELLY, R. J. & GLABERSON, W. 1966 Experiments on the capillary instability of a liquid jet. *Proc. R. Soc. Lond.* A **290**, 547–556.

DRAZIN, P. G. & REID, W. H. 1981 *Hydrodynamic Stability*. Cambridge University Press.

EGGERS, J. & DUPONT, T. F. 1994 Drop formation in a one-dimensional approximation of the Navier–Stokes equation. *J. Fluid Mech.* **262**, 205–221.

EGGERS, J. 1993 Universal pinching of 3D axisymmetric free-surface flow. *Phys. Rev. Lett.* **71**, 3458–3460.

EGGERS, J. 1995 Theory of drop formation. *Phys. Fluids* **7**, 941–953.

GOEDDE, E. F. & YUEN, M. C. 1970 Experiments on liquid jet instability. *J. Fluid Mech.* **40**, 495–511.

KELLER, J. B. 1983 Breaking of liquid films and threads. *Phys. Fluids* **26**, 3451–3453.

KELLER, J. B., KING, A. & TING, L. 1995 Blob formation. *Phys. Fluids* **7**, 226–228.

KELLER, J. B. & MIKSIS, M. J. 1983 Surface tension driven flows. *SIAM J. Appl. Maths* **43** (2), 268–277.

MANSOUR, N. & LUNDGREN, T. S. 1990 Satellite formation in capillary jet breakup. *Phys. Fluids* A **2**, 1141–1144.

PAPAGEORGIOU, D. T. 1994 Breakup of cylindrical jets governed by the Navier–Stokes equations. In *Proceedings of the Workshop on Transition, Turbulence and Combustion, June 7–July 2, 1993, ICASE/LaRC Interdisciplinary Series in Science and Engineering* (ed. M. Y. Hussaini, T. B. Gatski & T. L. Jackson), vol. 2, pp. 225–235. Kluwer.

PAPAGEORGIOU, D. T. 1995 On the breakup of viscous liquid threads. *Phys. Fluids* **7**, 1529–1544.

PEREGRINE, D. H., SHOKER, G. & SYMON, A. 1990 The bifurcation of liquid bridges. *J. Fluid Mech.* **212**, 25–39.

RAYLEIGH, LORD 1878 On the stability of jets. *Proc. Lond. Math. Soc.* **10**, 4–13.

RENARDY, M. 1994 Some comments on the surface-tension driven break-up (or the lack of it) of viscoelastic jets. *J. Non-Newtonian Fluid Mech.* **51**, 97–107.

STUART, J. T. 1960 On the nonlinear mechanics of wave disturbances in stable and unstable parallel flows. Part 1. The besic behaviour in plane Poiseuille flow. *J. Fluid Mech.* **9**, 353–370.

TAYLOR, G. I. 1959 The dynamics of thin sheets of fluid, I. Water bells. *Proc. R. Soc. Lond.* A **253**, 289–295.

TING, L. & KELLER, J. B. 1990 Slender jets and thin sheets with surface tension. *SIAM J. Appl. Maths* **50** (6), 1533–1546.

TJAHADI, M., STONE, H. A. & OTTINO, J. M. 1992 Satellite and subsatellite formation in capillary breakup. *J. Fluid Mech.* **243**, 297–317.

TOMOTIKA, S. 1935 On the stability of a cylindrical thread of a viscous liquid surrounded by another viscous fluid. *Proc. R. Soc. Lond.* A **150**, 322–337.

WATSON, J. 1960 On the nonlinear mechanics of wave disturbances in stable and unstable parallel flows. Part 2. The development of a solution for plane Poiseuille flow and plane Couette flow. *J. Fluid Mech.* **9**, 371–389.

YUEN, M.-C. 1968 Nonlinear capillary instability of a liquid jet. *J. Fluid Mech.* **33**, 151–163.

Note added in proof: Section 4 shows that Stokes theory is valid if $\tau^{\beta-2} \ll \tau^{-1-\beta}$ as $\tau \to 0$. This implies $\beta > \frac{1}{2}$ and not $\beta < \frac{1}{2}$ as written in §4. Since $\beta = 0.175$ the implication is that inertia is important near pinching and the solution of §4 takes over. I am grateful to Howard Stone and John Lister for pointing this out.